Galectin-3 Regulates a Molecular Switch from N-Ras to K-Ras Usage in Human Breast Carcinoma Cells

Ruby Shalom-Feuerstein,[1] Tomer Cooks,[1] Avraham Raz,[2] and Yoel Kloog[1]

[1]Department of Neurobiochemistry, George S. Wise Faculty of Life Sciences, Tel-Aviv University, Tel-Aviv, Israel and [2]Tumor Progression and Metastasis Program, Karmanos Cancer Institute, School of Medicine, Wayne State University, Detroit, Michigan

Abstract

Galectin-3 (Gal-3), a pleiotropic carbohydrate-binding protein, is a selective binding partner of activated K-Ras-GTP. Because both proteins are antiapoptotic and associated with cancer progression, we questioned the possible functional role of Gal-3 in K-Ras activation. We found that overexpression of Gal-3 in human breast cancer cells (BT-549/Gal-3) coincided with a significant increase in wild-type (wt) K-Ras-GTP coupled with loss in wt N-Ras-GTP, whereas the nononcogenic Gal-3 mutant proteins [Gal-3(S6E) and Gal-3(G182A)] failed to induce the Ras isoform switch. Only wt Gal-3 protein coimmunoprecipitated and colocalized with oncogenic K-Ras, resulting in its activation with radical alterations in Ras signaling pathway, whereby the activation of AKT and Ral was suppressed and shifted to the activation of extracellular signal-regulated kinase (ERK). Specific inhibitors for Ras or mitogen-activated protein/ERK kinase (farnesylthiosalicylic acid and UO126, respectively) inhibited Gal-3–mediated apoptotic resistance and anchorage-independent growth functions. In conclusion, this study shows that Gal-3 confers on BT-549 human breast carcinoma cells several oncogenic functions by binding to and activation of wt K-Ras, suggesting that some of the molecular functions of Gal-3 are, at least in part, a result of K-Ras activation. (Cancer Res 2005; 65(16): 7292-300)

Introduction

Gaining resistance to apoptosis and inducing uncontrolled cell growth are common characteristics often acquired by oncoproteins such as galectin-3 (Gal-3). This galactoside-binding protein is highly expressed in human neoplasma, including breast cancer. Recent studies have shown that overexpression of Gal-3 in breast tumor cells BT-549 confers protection against various apoptotic stimuli, including staurosporin, Adriamycin, and anoikis induction (1–3). Furthermore, it was suggested that Gal-3 phosphorylation at Ser^6 residue is required for its antiapoptotic activity, as a single amino acid substitution of serine at position 6 to alanine (S6A) resulted in loss of antiapoptotic function. Interestingly, Gal-3 contains the NWGR amino acid motif, a highly conserved sequence within the BH1 domain of Bcl-2 family proteins (3). To question whether this motif is critical to Gal-3 antiapoptotic activity, a single amino acid of Gly^{182} residue was substituted to alanine (G182A) by site-directed mutagenesis. This mutant also failed to prevent apoptosis when overexpressed in BT-549 cells. However, although it is evident that Gal-3 regulates apoptosis, the mechanism of how this antiapoptotic activity is accomplished is not clear.

Recent studies have shown that Gal-3 is a binding partner of K-Ras oncoprotein (4). This interaction promotes strong K-Ras activation (4). Ras proteins are commonly activated in human tumors either by point mutations or via uncontrolled cell surface receptor signaling (5). Activated Ras is capable of preventing apoptosis (6, 7) and promoting cell proliferation (8). In that way, the activities of Gal-3 are similar to those of oncogenic Ras. Therefore, we suspected that Gal-3 might carry out its biological functions through the activation of K-Ras. Here, we show that Gal-3 stimulation of antiapoptotic activity, cell proliferation, and anchorage-independent growth involves K-Ras/MEK [mitogen-activated protein/extracellular signal-regulated kinase (ERK) kinase] pathway.

Materials and Methods

Cell culture and transfection. The human breast cancer cell lines BT-549, BT-549/Gal-3[wild-type (wt)], BT-549/Gal-3(S6E), and BT-549/Gal-3(G182A) were established as described previously (1, 3). Rat intestinal epithelial (RIE-1) cells and RIE-1 cells stably expressing K-Ras(G12V) were established as described earlier (9, 10). BT-549, RIE-1, and COS-7 cell lines were grown at 37°C in DMEM containing 10% FCS, 100 μg/mL streptomycin, and 100 units/mL penicillin, and maintained in a humidified atmosphere of 95% air/5% CO_2. For the transfection, we plated 1×10^5 BT-549 cells on glass coverslips in six-well plates and transfected them with a total amount of 2 μg DNA using Fugene reagent according to the instructions of manufacturer (Roche Molecular Biochemicals, Mannheim, Germany). Immunofluorescence staining was carried out 48 hours after transfection as detailed below. COS-7 cells were grown in 10 cm dishes and 1.5×10^6 cells were transfected with 1 μg plasmid DNA coding for green fluorescent protein (GFP)-H-Ras(12V) or GFP-N-Ras(12V) or 2 μg plasmid DNA coding for GFP-K-Ras(12V) using dextran (Pharmacia, Stockholm, Sweden) as detailed elsewhere (4). Lysates obtained 48 hours after transfection were normalized and 30 μg protein were subjected to SDS-PAGE and Western immunoblotting as detailed below with either pan–anti-Ras antibody, anti–H-Ras antibody, anti–K-Ras antibody, anti–N-Ras antibody, or anti-GFP antibody and then with peroxidase–goat anti-mouse IgG (The Jackson Laboratory, Bar Harbor, ME). GFP-Ras vector constructs have been previously described (11, 12).

Western immunoblotting. Cells were washed with PBS and lysed with lysis buffer A [50 mmol/L Tris-HCl (pH 7.6), 20 mmol/L $MgCl_2$, 200 mmol/L NaCl, 0.5% NP40, 1 mmol/L DTT, and 1 mmol/L antiproteases]. Alternatively, particulated fractions were prepared by cell resuspension using buffer B (buffer A with no detergent), sonication, and ultracentrifugation at $100,000 \times g$ for 30 minutes followed by pellet resuspension with buffer B and sonication. Lysates or particulated fractions were subjected to SDS-PAGE, followed by immunoblotting with one of the following antibodies as described: 1:2,500 pan-Ras antibody; 1:20 anti–H-Ras antibody; 1:20 anti–K-Ras antibody; 1:20 anti–N-Ras antibody; 1:500 antitubulin antibody; 1:500 anti–Gal-3 antibody; 1:500 anti-GFP antibody; 1:2,000 anti-ERK antibody; 1:10,000 anti–phospho-ERK antibody; 1:1,000 anti-Akt antibody; 1:1,000 anti–phospho-Akt antibody; or 1:1,000 anti-Ral antibody.

Note: Y. Kloog is an incumbent of The Jack H. Skirball Chair in Applied Neurobiology.

Requests for reprints: Yoel Kloog, Department of Neurobiochemistry, George S. Wise Faculty of Life Sciences, Tel-Aviv University, 69978 Tel-Aviv, Israel. Phone: 972-3-640-9699; Fax: 972-3-640-7643; E-mail: yoelk@tauex.tau.ac.il.

©2005 American Association for Cancer Research.

doi:10.1158/0008-5472.CAN-05-0775

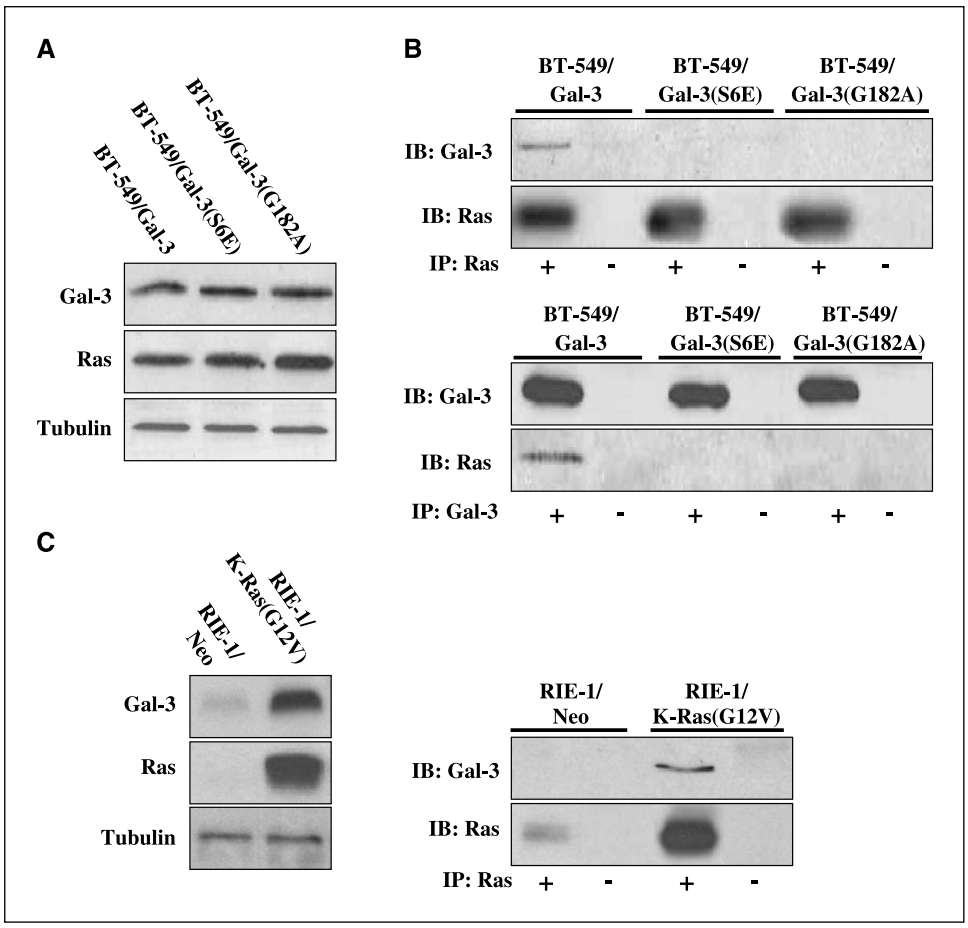

Figure 1. The association of Ras and galectin-3. Lysates of BT-549 or of RIE-1 cell variants were immunoprecipitated (*IP*) then immunoblotted with either pan–anti-Ras antibody (*IB: Ras*) or with anti–Gal-3 antibody (*IB: Gal-3*) as detailed in Materials and Methods. *A,* BT-549 cell samples were subjected to SDS-PAGE and (*B*) was precipitated with anti–Gal-3 antibodies and probed (immunoblotting) with anti-Ras antibodies or precipitated with anti-Ras and probed with anti–Gal-3 antibodies. The endogenous levels of Ras and of Gal-3 in the cell extracts are shown in (*A*) and loading control was determined by the level of β-tubulin. *C,* RIE-1 and RIE-1/K-Ras(G12V) cell samples were subjected to SDS-PAGE followed by immunoblotting with anti-Ras or anti–Gal-3 antibodies (*left*), or precipitated with anti-Ras antibody and probed with anti-Ras and anti–Gal-3 antibodies (*right*). Naive IgG served as controls (−) for immunoprecipitation with the specific antibody (+).

Immunoblots were then exposed either to 1:5,000 peroxidase–goat anti-mouse IgG or to 1:5,000 peroxidase–goat anti-rabbit IgG or to 1:5,000 peroxidase–goat anti-rat IgG and protein bands were visualized by enhanced chemiluminescence (ECL) and quantified by densitometry with Image Master VDS-CL (Amersham Pharmacia Biotech, Arlington Heights, IL) using TINA 2.0 software (Ray Tests). ECL kit was from Amersham. Rat anti–Gal-3 antibody was from Roche Molecular Biochemicals; mouse anti–pan-Ras antibody (Ab-3) was from Calbiochem (La Jolla, CA); isoform-specific mouse anti-Ras antibodies, mouse anti–phospho-ERK antibody, and mouse antitubulin antibody (AK-15) were from Sigma-Aldrich (St. Louis, MO); rabbit anti-ERK1/2 antibody and mouse anti-GFP antibody were from Santa Cruz Biotechnology (Santa Cruz, CA); rabbit anti–phospho-Akt antibody (Ser^{473}; 4E2) and rabbit anti-Akt antibody was from Cell Signaling (Beverly, MA); rabbit anti–PI3-K p85 antibody was from Upstate Biotechnology (Lake Placid, NY); peroxidase–goat anti-mouse IgG, peroxidase–goat anti-rat IgG, and peroxidase–goat anti-rabbit IgG were from Jackson ImmunoResearch Laboratories (West Grove, PA); and mouse anti-Ral antibody was from Transduction Laboratories (Los Angeles, CA).

Coimmunoprecipitation and Ras-GTP assays. Cell lysates containing 6 and 1 mg proteins were prepared using lysis buffer A for coimmunoprecipitations or Ras-binding domain of Raf-1 (RBD) assays, respectively. For immunoprecipitations, 6 mg protein adjusted to a total volume of 1 mL were immunoprecipitated for 1 hour with 3 μg mouse pan-Ras antibody or 30 μL rat anti–Gal-3 antibody (4) and 30 μL sheep anti-mouse iron beads or sheep anti-rat iron beads (Dynal Biotech, Los Angeles, CA), respectively. Samples were precipitated using magnetic field and washed with lysis buffer and prepared for SDS-PAGE and Western immunoblotting with either 1:2,500 pan–anti-Ras antibody and 1:5,000 peroxidase–goat anti-mouse IgG or 1:500 rat anti–Gal-3 antibody and 1:5,000 peroxidase–goat anti–rat IgG (The Jackson Laboratory). Lysates containing 1 mg protein were used for the determination of Ras-GTP by the glutathione *S*-transferase (GST)-RBD pull-down assay as described (4), followed by Western immunoblotting with pan–anti-Ras antibody or with isoform-specific anti-Ras antibodies as detailed above.

Confocal microscopy. We plated cells on glass coverslips, then transfected the cells with 2 μg plasmid DNA coding for GFP-K-Ras(12V) as described above. The transfected cells were stained for Gal-3 as described in details (4). Briefly, cells were fixed permeabilized and then labeled with rat Gal-3 antibody followed by incubation with biotin–goat anti-rat IgG and Cy3-streptavidin (Jackson ImmunoResearch, West Grove, PA). The cells were then analyzed with a Zeiss LSM 510 confocal microscope fitted with nonleaking green and red fluorescence filters and colocalization was assessed by the colocalization function of the LSM 510 software, as described (11).

Phosphoinositide 3-kinase activity and Ral-GTP assays. Cells were grown in 10 cm dishes to 80% confluence. For determining phosphoinositide 3-kinase (PI3K) activity, we lysed the cells using PI3K lysis buffer (4, 13), then 1 mg protein of each sample was adjusted to a volume of 500 μL. The enzyme was immunoprecipitated by incubation with rabbit anti-PI3K p85 antibody (Upstate Biotechnology), and its activity was assayed with 0.5 mg/mL phosphatidylinositol and 125 μmol/L ATP and 5 μCi of [γ-^{32}P]ATP. We extracted the lipids with chloroform/methanol and then separated them by thin layer chromatography (4, 13). Phospholipid markers were used for the identification of the ^{32}P-labeled phosphatidylinositol 3-phosphate product (4, 13). The ^{32}P-labeled lipid products were visualized by an overnight exposure on an X-ray film, and the spots were then quantified by TINA analysis. For the determination of Ral-GTP levels, we lysed the cells with Ral-GTP lysis buffer (pH 7.5), then 0.5 mg protein of each sample was adjusted to a volume of 500 μL. The Ral-GTP pull down was obtained using GST-Ral binding domain–coated beads prepared as

detailed previously (14), followed by Western immunoblotting with anti-Ral antibody.

Cell proliferation and drug resistance assays. We planted 5×10^4 cells in six-well plates for the cell proliferation assays. After 5 hours, 75 μmol/L farnesylthiosalicylic acid (FTS) or 30 μmol/L UO126 or the vehicle 0.1% Me_2SO were added. Cell proliferation was determined after 4 days by using the 3-(4,5-dimethylthiazol-2-yl)-2,5-diphenyltetrazolium bromide (MTT) assay, which determines mitochondrial activity in living cells. The cells were incubated with 0.1 mg/mL MTT for 2 hours at 37°C then lysed with 100% Me_2SO. Results were quantified by reading the absorbance at 570 to 630 nm. We planted 2,500 cells in 96-well plates for the drug resistance assays. At the next day, 75 μmol/L FTS or 30 μmol/L UO126 or the vehicle 0.1% Me_2SO were added. After 10 hours of preincubation with the inhibitors, 10 μmol/L Adriamycin or 500 nmol/L staurosporine or vehicles were added for 24 hours followed by viability evaluation using MTT as described above. For the fluorescence-activated cell sorting (FACS) analysis, we planted 1×10^6 cells in 10 cm dishes. The next day, 75 μmol/L FTS or 30 μmol/L UO126 or the vehicle 0.1% Me_2SO were added. After 10 hours of preincubation with the inhibitors, 10 μmol/L Adriamycin or 500 nmol/L staurosporine were added for 36 or for 2.5 hours, respectively. Cells were then collected and suspended with PBS containing propidium iodide (50 μg/mL; Sigma) and 0.05% Triton X-100 (BDH, Poole, United Kingdom) for nuclear staining, then analyzed with a fluorescence-activated cell sorter (FACSCalibur, Becton Dickinson, Los Angeles, CA).

Anchorage-independent growth. We planted 200 suspended cells in 50 μL DMEM containing 10% FCS and 0.5% agarose on the top of 50 μL DMEM containing 10% FCS and 1% soft agarose that had been allowed to gel previously at 96-well plates. The dishes were incubated at 37°C for ~3 weeks. Then, 25 μL MTT was added for 4 hours and colonies were visualized and counted.

Results

Gal-3, but not Gal-3 mutants lacking antiapoptotic activity, interacts with Ras. We postulated that the antiapoptotic effects of Gal-3 in BT-549 cells could be associated with Ras–Gal-3 interactions and thus examined whether Ras and Gal-3 expressed in BT-549/Gal-3 cells interact with each other. Total BT-549/Gal-3 cell lysates were used for coimmunoprecipitation assays in which either Ras proteins were immunoprecipitated with pan–anti-Ras antibody then immunoblotted with anti–Gal-3 antibody or Gal-3 was immunoprecipitated with anti–Gal-3 antibody then immunoblotted with pan-Ras antibody. To gain more support for the hypothesis that Ras–Gal-3 interactions may promote antiapoptotic signals in BT-549 cells, negative controls of lysates of BT-549 cells stably expressing Gal-3 mutants that lack antiapoptotic activity [Gal-3(S6E) and Gal-3(G182A)] were used as well. All cell lines used expressed similar amounts of Gal-3(wt) or its mutants and Ras (Fig. 1*A*). Results of a typical experiment (Fig. 1*B*) show that Ras and Gal-3 coimmunoprecipitated from lysates of BT-549/Gal-3 cells; pan–anti-Ras antibody pulled down Gal-3 and anti–Gal-3 antibody pulled down Ras. Naive antibodies failed to immunoprecipitate either Ras or Gal-3 (Fig. 1*B*). Importantly, Ras did not coimmunoprecipitate with Gal-3(S6E) or Gal-3(G182A), which for themselves immunoprecipitated well with anti–Gal-3Ab (Fig. 1*B*). Similarly, although equal amount of Ras were immunoprecipitated from lysates of all BT-549 cell lines with anti-Ras antibody, Gal-3 was not pulled down by the pan–anti-Ras antibody from lysates of BT-549/Gal-3(S6E) or BT-549/Gal-3(G182A) cells (Fig. 1*B*). These observations were not unique to BT-549/Gal-3 cells because Ras and Gal-3 coimmunoprecipitated from lysates of RIE-1 cells stably expressing K-Ras(G12V) (Fig. 1*C*). Apparently, expression of this oncogenic Ras isoform in RIE-1 cells induced an increase in Gal-3 expression (Fig. 1*C*) and rendered them resistant to apoptosis (9, 10).

Next, we examined the possibility that Gal-3 and K-Ras are colocalized in BT-549/Gal-3 cells. In these experiments, we transfected each of the BT-549 cell type with GFP-K-Ras(12V) and examined by dual-fluorescence confocal microscopy whether Gal-3 and its mutants colocalize with the transiently expressed constitutively active GFP-K-Ras(12V) protein. We used this Ras isoform because earlier experiments showed that among various Ras isoforms (H-, K-, and N-Ras), only activated K-Ras interacted with Gal-3 (4). Typical images of this experiment show that GFP-K-Ras(12V) [green fluorescence] and Gal-3, but not Gal-3(S6E) or Gal-3(G182A) [stained with anti–Gal-3 antibody, red fluorescence], colocalized in the cell membrane (Fig. 2*A* and *B*). These results, along with those obtained in the coimmunoprecipitation experiments, pointed to the possibility that Gal-3 interacts with the active

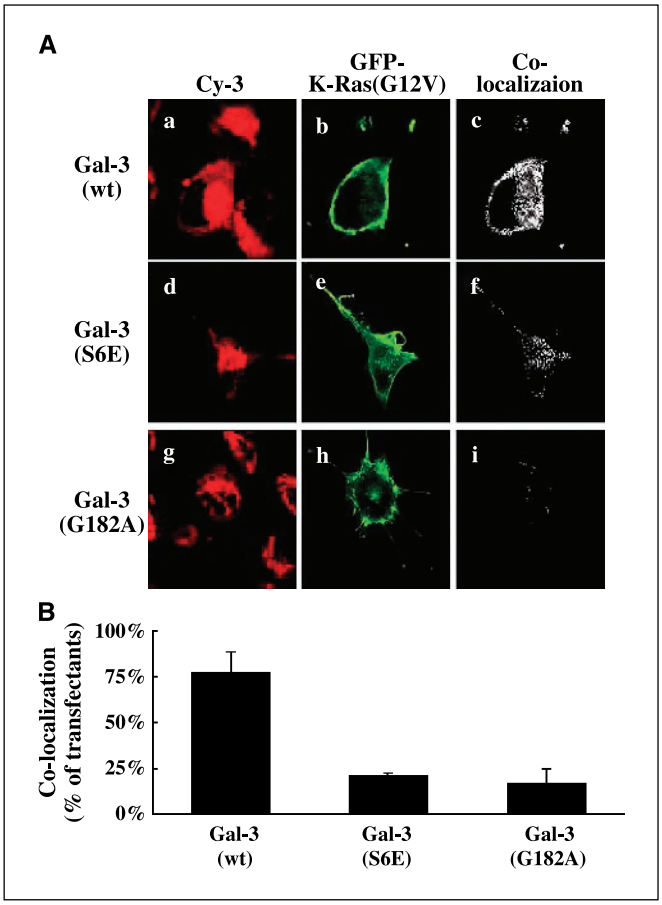

Figure 2. Active K-Ras–Gal-3 interaction. Cells were cultivated for 48 hours, washed with PBS, fixed, and processed for confocal microscopy. *A,* BT-549 stably expressing Gal-3(wt) (*a*, *b*, *c*), Gal-3(S6E) (*d*, *e*, *f*), and Gal-3(G182A) (*g*, *h*, *i*) were transfected with DNA plasmids encoding for GFP-K-Ras(G12V) in six-well plates. After 48 hours, Gal-3 protein was detected using Cy-3 fluorophore as detailed in Materials and Methods. Similar images were collected from 10 cells in each well. Colocalization was assessed by dual-image confocal microscopy [green fluorescence for GFP-K-Ras(G12V), red for Gal-3]. Typical images of Gal-3 (*a*, *d*, *g*), GFP-K-Ras(G12V) (*b*, *e*, *h*), and the extent of colocalization (*c*, *f*, *i*) show colocalization of Gal-3 and GFP-K-Ras(G12V) at the plasma membrane. No such colocalization is observed in the GFP-K-Ras(G12V)/Gal-3(S6A) or GFP-K-Ras(G12V)/Gal-3(G182A) cells. *B,* quantification of the colocalization of Gal-3 and active K-Ras. The percentages of transfectant cells in (*A*) that display colocalization were calculated in a blind fashion of all transfectants. Similar images were collected from 10 to 12 cells in each series of transfection.

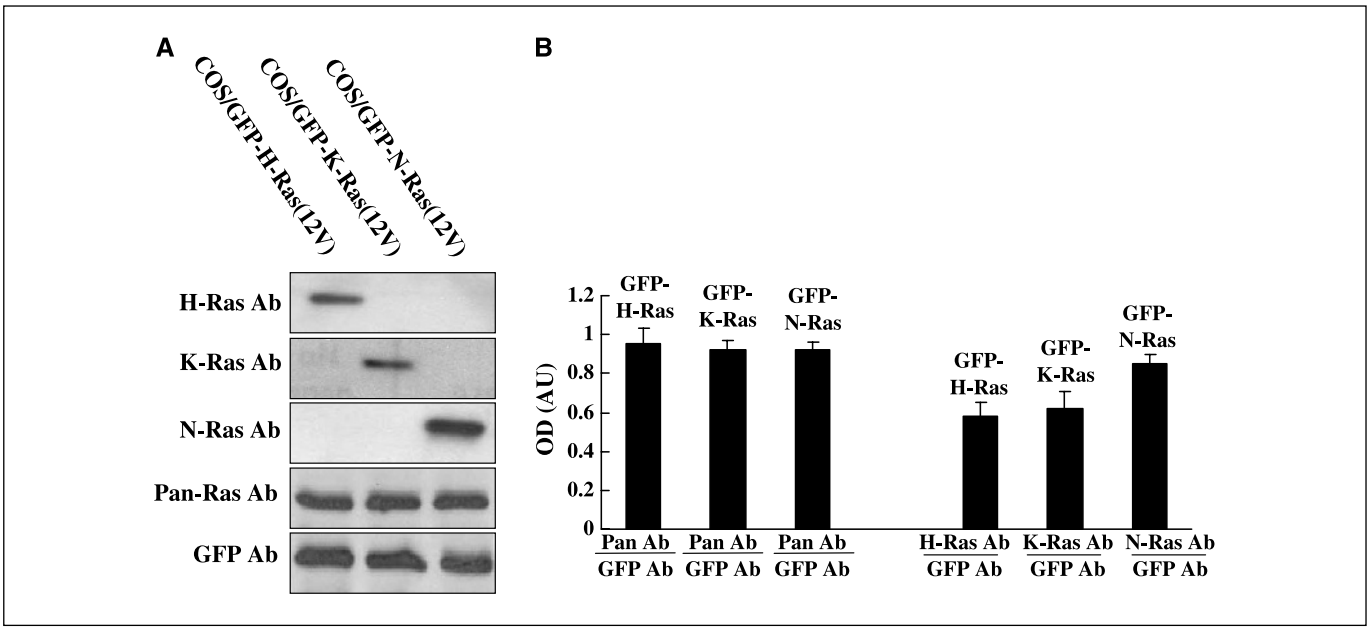

Figure 3. Ras isoform–specific antibodies. COS-7 cell were transfected with the GFP-Ras(12V) constructs encoding the indicated GFP-Ras isoforms. Cell lysates were subjected to Western analysis with either pan–anti-Ras antibody (*Pan-Ras Ab*) or Ras isoform–specific antibodies or anti-GFP antibody followed by densitometric tracing as detailed in Materials and Methods. *A,* typical immunoblots. *B,* the sensitivity of each of the Ras isoform–specific antibody was then estimated as the ratio between the optical densities obtained from blotting with Ras isoform–specific antibody and that obtained by blotting with anti-GFP antibodies. The ratios were then used as normalizing factors in the determination of levels of expression and the levels of activation of the various Ras isoforms in BT-549 cell lines. The ratio between the absorbance obtained by immunoblotting with pan-Ras antibody and that obtained with anti-GFP antibodies (*B*, *left*) shows equal sensitivity of pan-Ras antibody to all Ras isoforms. *Columns,* means (n = 3); *bars,* SD.

wt K-Ras isoform expressed in BT-549 cells. Such an interaction would lead to a shift in K-Ras–GTP/K-Ras–GDP steady-state toward K-Ras–GTP (4).

Levels of expression of Ras isoforms in BT-549 cell lines. The proposition that Gal-3 expression induced K-Ras activation could be assessed by determining the levels of expression of each Ras isoform in the various BT-549 cell lines. We thus used Ras isoform–specific antibodies (anti–H-Ras, anti–K-Ras, and anti–N-Ras antibodies). Specificity and sensitivity of each of the antibodies was determined by immunoblotting using extracts of COS-7 cells expressing comparable amounts (assessed with anti-GFP antibody) of GFP-tagged H-Ras, K-Ras, and N-Ras (Fig. 3). Unlike the pan–anti-Ras antibody that reacted equally well with all GFP-tagged Ras proteins, the Ras isoform–specific antibodies displayed diverse

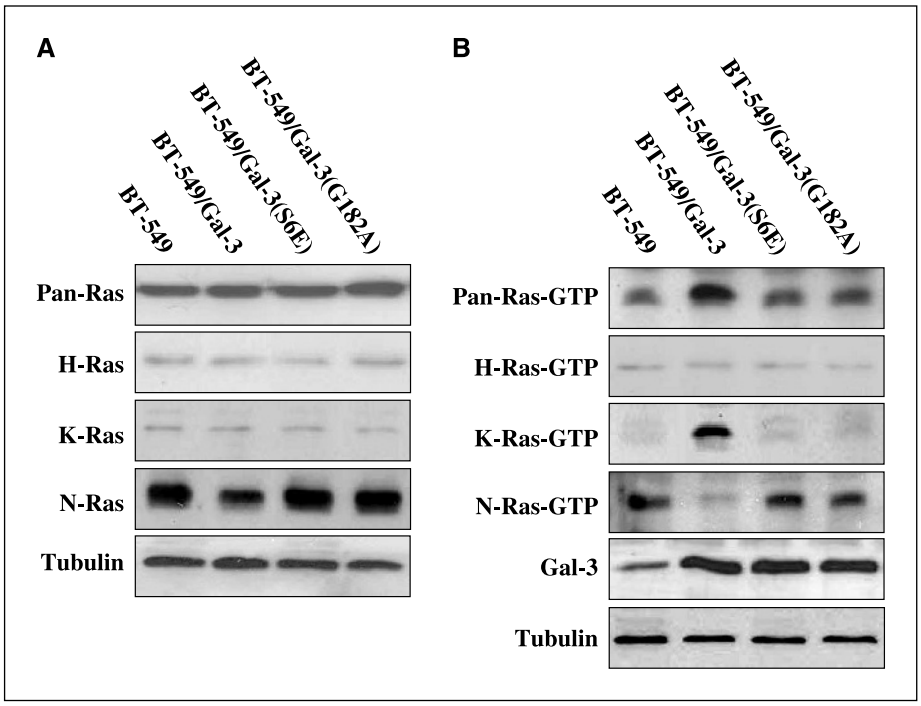

Figure 4. Galectin-3–induced K-Ras activation at the expense of N-Ras in BT-549 cells. *A,* the levels of Ras or H-Ras, K-Ras, and N-Ras isoform proteins in particulated fractions was established by Western analysis utilizing pan-Ras antibody or with Ras isoform–specific antibodies, respectively. *B,* the expression levels of Ras-GTP (all Ras isoforms), H-Ras-GTP, K-Ras-GTP, and N-Ras-GTP in the indicated cell lysates using the RBD Ras-GTP pull-down method followed by blotting with either pan–anti-Ras antibody (Ras-GTP) or with Ras isoform–specific antibodies. The levels of expression of Gal-3 were determined for all cell lysates by immunoblotting with anti–Gal-3 to verify comparable Gal-3 levels expressed in the various stable Gal-3 cell lines. Anti–β-tubulin antibody was used for protein loading control. Immunoblots of one of three experiments with similar results are shown. Statistical analysis is given in Tables 1 (Ras) and 2 (Ras-GTP).

sensitivities (Fig. 3*A* and *B*). Although each of the antibodies reacted only with the corresponding GFP-Ras protein, the anti–N-Ras antibody exhibited high sensitivity toward GFP–N-Ras, whereas the anti–H-Ras and anti–K-Ras antibodies exhibited relatively low sensitivities toward the corresponding GFP-tagged Ras isoforms (Fig. 3*A*). The ratio of the absorbance of each GFP-Ras protein band determined with the Ras isoform–specific antibody and that determined with the anti-GFP antibody (Fig. 3*B*) was then used as a factor to correct for antibody sensitivity (see details in legend to Fig. 3).

This practice enabled us to determine the levels of expression of each Ras isoform in the various BT-549 cell lines. The particulate fractions of the cells were immunoblotted either with pan-Ras antibody or with Ras isoform–specific antibodies (Fig. 4*A*) and the apparent levels of expression of each isoform were estimated using the above noted correction factors (Table 1). This analysis showed that N-Ras is the most abundant Ras isoform in BT-549 cells (75% of total Ras proteins), where H-Ras and K-Ras were expressed at similar low levels (12% and 12% of total Ras proteins, respectively). A similar Ras immunoblot analysis done with BT-549/Gal-3 cells showed that Gal-3 did not affect the levels of expression of H-Ras or K-Ras, yet it induced a small decrease (21.6 ± 9%, mean ± SD, $P < 0.05$) in the levels of expression of N-Ras (Fig. 4*A*). No differences were observed between the levels of expression of Ras isoforms in BT-549 cells and BT-549/Gal-3(S6E) or BT-549/Gal-3(G182A) cells (Fig. 4*A*; Table 1). Thus, Gal-3 or its mutants had no major effect on the levels of expression of Ras proteins (pan-Ras antibody; see Fig. 4*A*) or on the relative levels of expression of each of the Ras isoforms.

Gal-3 induces K-Ras activation at the expense of N-Ras in BT-549 cells. Next, we examined the possible impact of Gal-3 on Ras activation in the various BT-549 cell lines determining the levels of Ras-GTP. The active Ras protein was pulled down from cell lysates by GST-RBD and then determined by immunoblotting with pan-Ras antibody. We found that BT-549 cells exhibit small but significant amounts of active Ras-GTP accounting for 3 ± 1% (mean ± SD, $n = 3$) of total Ras protein expressed by the cells (Fig. 4*B*; Table 2). Expression of Gal-3, but not of Gal-3(S6E) or Gal-3(G182A), induced a marked increase in Ras-GTP; the levels of Ras-GTP in BT-549/Gal-3 cells were 12 ± 3% (mean ± SD, $n = 3$), remarkably higher than those of BT-549 cells ($P < 0.01$; Fig. 4*B*; Table 2).

Table 1. Levels of expression of Ras isoforms in BT-549 cell lines

Cell line/Ras isoform	BT-549	BT-549/ Gal-3(wt)	BT-549/ Gal-3(S6E)	BT-549/ Gal-3(G182A)
H-Ras	12 ± 2%	13 ± 3%	11 ± 3%	11 ± 3%
K-Ras	12 ± 3%	16 ± 2%	15 ± 3%	14 ± 4%
N-Ras	75 ± 6%	71 ± 6%	75 ± 4%	74 ± 8%

NOTE: Levels of expression of Ras isoforms in BT-549, BT-549/Gal-3, BT-549/Gal-3(S6E), and BT-549/Gal-3(G182A) cells were determined by Western immunoblotting using Ras isoform–specific antibodies as detailed in Fig. 3 and in the text. Data represent the apparent amount of each Ras isoform in the various cell lines in terms of percentage of the total amount of all Ras isoforms (means ± SD, $n = 3$).

Table 2. Levels of active Ras-GTP proteins in BT-549 cell lines

Cell line/Ras isoform	BT-549	BT-549/ Gal-3(wt)	BT-549/ Gal-3(S6E)	BT-549/ Gal-3(G182A)
Pan-Ras	3 ± 1%	12 ± 3%	3 ± 1%	4 ± 2%
H-Ras	4 ± 2%	5 ± 2%	5 ± 2%	4 ± 1%
K-Ras	2 ± 1%	27 ± 3%*	2 ± 1%	3 ± 1%
N-Ras	7 ± 3%	2 ± 1%	8 ± 3%	8 ± 2%

NOTE: Levels of Ras-GTP in BT-549, BT-549/Gal-3, BT-549/Gal-3(S6E), and BT-549/Gal-3(G182A) cells were determined by the RBD pull-down assay followed by Western immunoblotting with pan-Ras antibody or with Ras isoform–specific antibodies as detailed in Fig. 4 and in the text. Data (means ± SD, $n = 3$) represent the apparent amount of Ras-GTP in terms of percentage of the total amount of Ras protein as determined with pan-Ras antibody or with Ras isoform–specific antibodies.
*$P < 0.05$ compared with BT-549 cells.

To reveal whether the high Ras-GTP levels observed in BT-549/Gal-3 cells corresponds to a specific Ras isoform, we pulled down Ras-GTP with GST-RBD and then determined the levels of each of the GTP-bound Ras protein by immunoblotting with the Ras isoform–specific antibody. We found that the most abundant active Ras isoform in BT-549 cells was N-Ras (Fig. 4*B*). N-Ras-GTP accounted for 7 ± 3% of total N-Ras protein; H-Ras-GTP accounted for 4 ± 2% of total H-Ras protein; and K-Ras-GTP accounted for 2 ± 1% of total K-Ras protein in BT-549 cells (mean ± SD, $n = 3$; Table 2). Expression of Gal-3, not of its inactive mutants, induced a marked increase in active K-Ras-GTP; the levels of K-Ras-GTP in BT-549/Gal-3 cells were 23.5 ± 2–fold higher than in BT-549 cells ($P < 0.05$; Fig. 4*B*). K-Ras-GTP in BT-549/Gal-3 accounted for 27 ± 3% (mean ± SD, $n = 3$) of total K-Ras protein expressed by the cells, emphasizing the strong activation of this Ras isoform by Gal-3. By marked contrast, N-Ras activation was strongly reduced by Gal-3 expression (Fig. 4*B*; Table 2). Gal-3 had no effect on H-Ras-GTP levels, which were relatively low in all BT-549 cell lines (Fig. 4*B*; Table 2). These experiments showed that Gal-3 induced a complete shift in Ras isoform usage in BT-549 cells. Because the two Gal-3 mutants that lack antiapoptotic activity (1, 2) failed to induce a Ras isoform switch in BT-549 cells (Fig. 4*B*; Table 2), it seems that the N-Ras to K-Ras switch contributes to the antiapoptotic effects of Gal-3 in BT-549 cells presumably due to alterations in Ras signaling (15).

Gal-3 augmentation of BT-549 cell transformation depends on Ras and ERK. Thus, we examined the levels of activation of ERK, Akt, and Ral as readouts of the prominent Ras effectors Raf, PI3-K, and RalGEF, respectively. We found that the levels of the active ERK (phospho-ERK) were significantly higher in BT-549/Gal-3 cells compared with those observed in BT-549 cells (2.9 ± 0.4 fold higher; Fig. 5*A* and *B*). By marked contrast, the levels of the active Akt (phospho-Akt) and of the active Ral (Ral-GTP) were far lower in BT-549/Gal-3 cells compared with those observed in BT-549 cells (presenting 9 ± 1% and 6 ± 1% of the levels recorded in BT-549-cells, respectively; Fig. 5*A* and *B*). Such alterations in Ras signals were not observed in BT-549 cells expressing the inactive Gal-3 mutants (Fig. 5*A* and *B*). These results suggested that the Gal-3 induced K-Ras activation that is

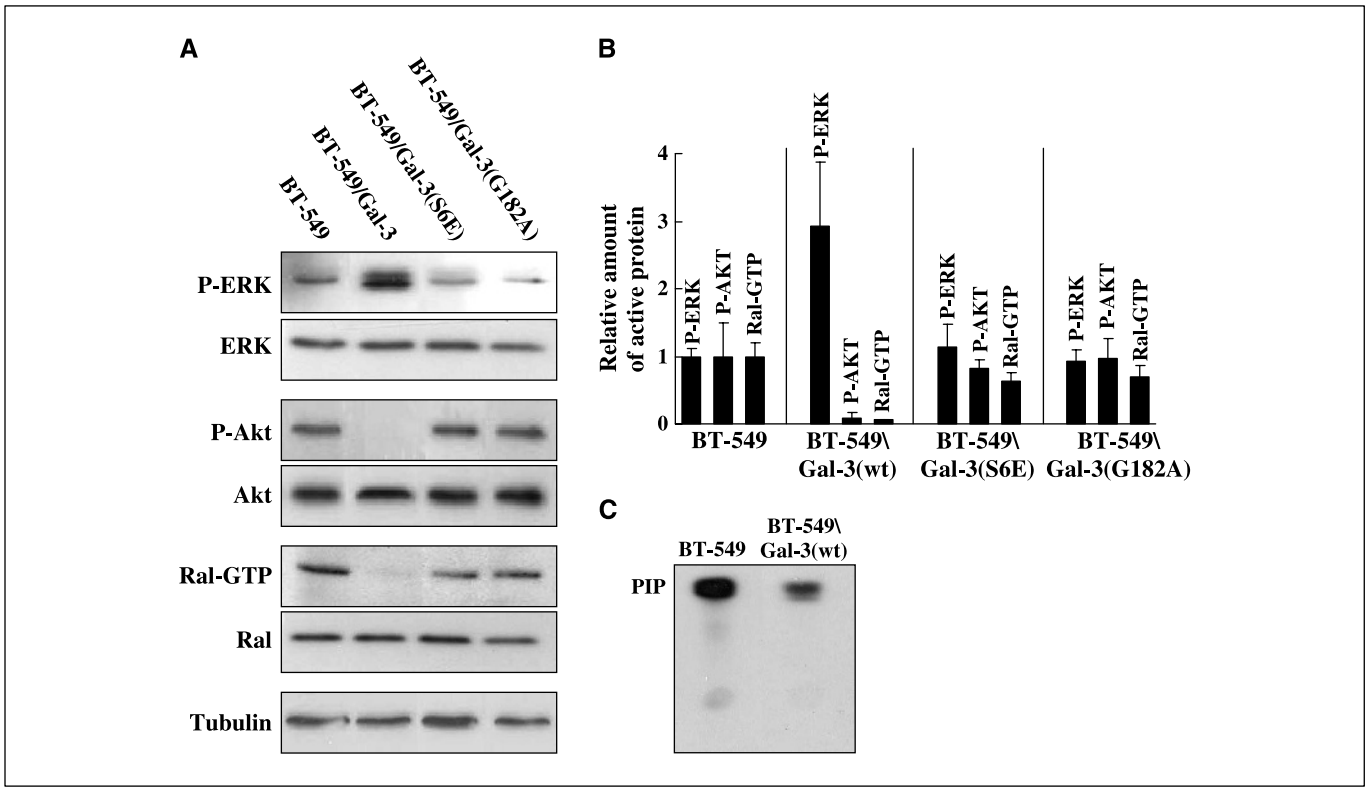

Figure 5. Ras signaling. *A,* cell lysates from the indicated cell variant were extracted and the total amounts of phosphorylated (active) ERK (*P-ERK*), total ERK (*ERK*), phosphorylated (active) AKT (*P-Akt*), total AKT (*Akt*), and total Ral (*Ral*) were determined by Western analysis with the suitable antibodies. Alternatively, 0.5 mg protein was used for Ral-GTP pull-down method followed by immunoblotting with anti-Ral antibody. Anti–β-tubulin antibody was used to guarantee accurate protein loading. *B,* results of representative experiments quantified by densitometry analysis. *Columns,* mean values recorded in BT-549 cells relative with those recorded in the cell variants (n = 3); *bars,* SD. *C,* lysates extracted from BT-549 Gal-3 (null cells) and BT-549/Gal-3 were immunoprecipitated with anti–PI3-K p85 antibody; PI3-K activity was then determined. The phosphatidylinositol-3-phosphate (*PIP*) ^{32}P-labeled lipid products were separated by thin layer chromatography and autoradiographed overnight. Similar results were obtained in two additional experiments.

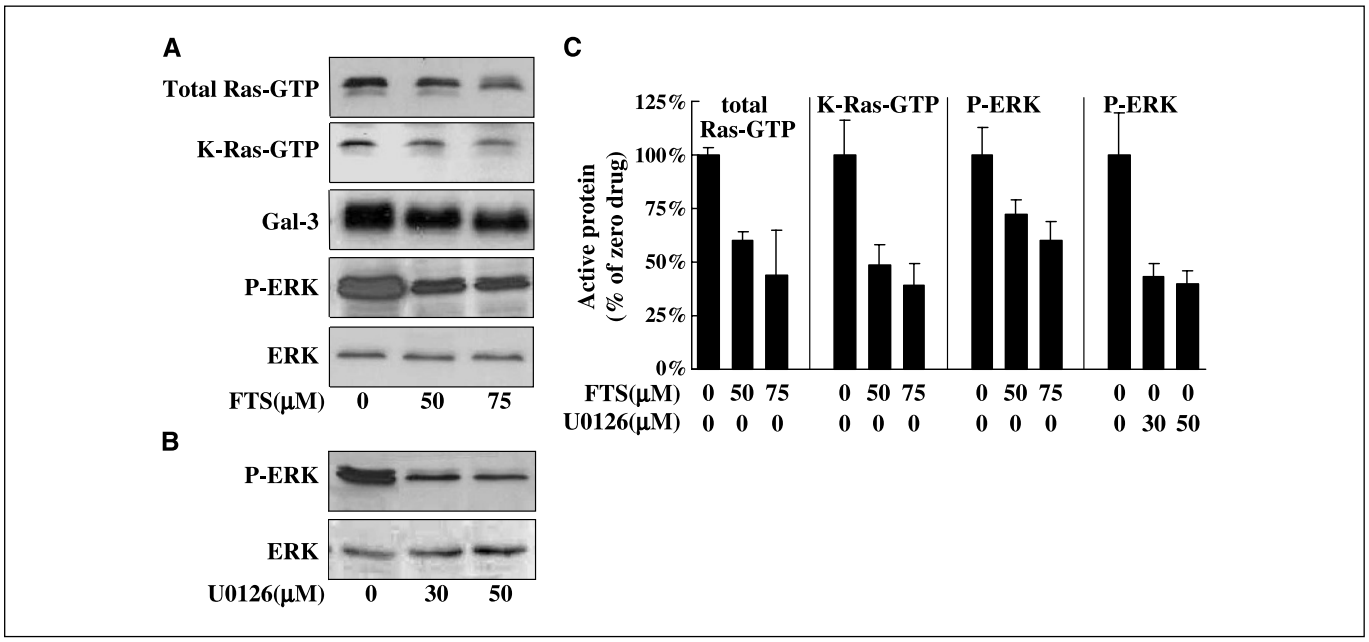

Figure 6. Inhibition of Ras and MEK. *A,* BT-549/Gal-3 cells were cultivated for 24 hours in the presence of the indicated concentrations of the Ras inhibitor FTS (*A*) or the MEK inhibitor UO126 (*B*). Subsequently, the cells were lysed and subjected to RBD Ras-GTP pull-down method followed by immunoblotting with either pan–anti-Ras antibody (*Total Ras-GTP*) or with Ras isoform–specific antibodies. Alternatively, lysates were immunoblotted against Gal-3, phosphorylated (active) ERK, total ERK, or against β-tubulin, which was used for protein loading control. Results of representative experiments are shown. *C,* quantification of (*A*) and (*B*) by densitometry analysis. *Columns,* means (n = 3); *bars,* SD.

accompanied by reduced N-Ras activation in BT-549/Gal-3 cells promoted a strong Ras-Raf-MEK-ERK signal on the expense of activation of PI3-K and of RalGEF. Evidently, PI3-K activity was 77 ± 9% lower in BT-549/Gal-3 cells compared with that recorded in BT-549 cells (Fig. 5*C*).

Therefore, we examined whether inhibition of active Ras or of ERK activation can reverse the Gal-3–induced aggressive phenotype of BT-549/Gal-3 cells, which is manifested *inter alia* by enhanced cell proliferation, anchorage-independent cell growth, and by resistance to cytotoxic drugs and anoikis (1, 2, 16, 17). In these experiments, we used the Ras inhibitor FTS and the MEK inhibitor UO126. Consistent with earlier studies in a variety of tumor cell lines (18, 19), we found that FTS caused a marked reduction in total active Ras protein and in active K-Ras in BT-549/Gal-3 cells (56 ± 15 and 61 ± 11% reduction at 75 μmol/L FTS, respectively; Fig. 6*A* and *C*). Concomitantly, the levels of phospho-ERK were down-regulated as well (40 ± 9% reduction at 75 μmol/L FTS; Fig. 6*A* and *C*). Similarly, the MEK inhibitor UO126 induced strong inhibition of ERK phosphorylation in BT-549/Gal-3 cells (60 ± 6% reduction at 50 μmol/L UO126; Fig. 6*B* and *C*). Along with the inhibition of Ras and ERK by FTS or of ERK by UO126, the anchorage-dependent (Fig. 7*A*) and the anchorage-independent (Fig. 7*B* and *C*) growth of BT-549/Gal-3 cells were strongly inhibited. Evidently, the Ras and MEK inhibitors reduced BT-549/Gal-3 cell growth to a level close to that observed in BT-549 cells (Fig. 7).

We then examined the effects of FTS and of UO126 on the cytotoxic effects of Adriamycin and staurosporine in BT-549/Gal-3 cells using the MTT cell viability assay and FACS analysis. Previous studies showed that BT-549/Gal-3 cells are more resistant to these cytotoxic drugs than BT-549 cell (Fig. 8*A* and *B*; refs. 1–3). Thus, we exposed BT-549/Gal-3 cells to 10 μmol/L Adriamycin or 0.5 μmol/L staurosporine in the presence or in the absence of 75 μmol/L FTS or 30 μmol/L UO126, which for themselves had no cytotoxic effects (Fig. 8*C* and *D*). The apparent cell death induced by 10 μmol/L Adriamycin (9 ± 4%) was increased to the levels of 30 ± 5% and 27 ± 7% in the presence of 75 μmol/L FTS and 30 μmol/L UO126, respectively (Fig. 8*C*). The inhibitors also induced similar increases in the number of cells in sub-G_1 phase (indicative of apoptotic cells; Fig. 8*D*). The death induced by 0.5 μmol/L staurosporine (39 ± 3%) was increased to the levels of 61 ± 5% and 58 ± 7% in the presence of 75 μmol/L FTS and 30 μmol/L UO126, respectively (Fig. 8*C*); the inhibitors also augmented the staurosporine-induced increase in number of cells in sub-G_1 phase (Fig. 8*D*). Taken together, these experiments strongly suggest that Gal-3 augmentation of BT-549 cell transformation depends, at least in part, on K-Ras and ERK.

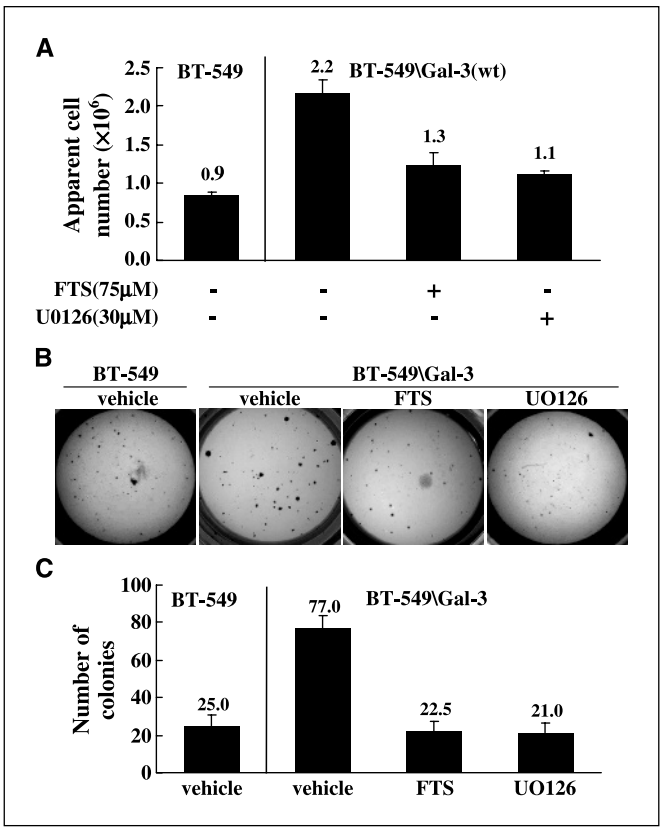

Figure 7. Transformed phenotype of cells is Ras and MEK dependent. *A,* the indicated cells were seeded in six-well plates. After 4 hours, specific inhibitors against Ras or MEK were added (+), or vehicle (−) was added as control. Cells were cultivated for additional 4 days and then counted. *B,* the indicated cells were plated in soft agarose (in 96-well plates as detailed in Materials and Methods), in the presence of the Ras inhibitor (75 μmol/L) FTS or the MEK inhibitor (30 μmol/L) UO126 or vehicle as control. After 21 days of incubation, MTT was added for 4 hours and colonies were visualized. *C,* number of colonies in each treatment was scored using the computerized Image-Pro software. Quantified results of a typical experiment are shown. *Columns,* mean; *bars,* SD.

Discussion

Gal-3, which is expressed at relatively high levels in a large number of human neoplasms (16), contributes to the maintenance of the malignant phenotype of the tumor cells (20). Such cancerous cells that express high levels of Gal-3 exhibit elevated growth rates, enhanced metastasis, resistance to anoikis, and resistance to apoptosis induced by cytotoxic drugs (1, 2, 16, 17). Gal-3 is a pleiotropic protein with activities mediated by sugar-protein interactions through the binding of Gal-3 to extracellular β-galactoside–binding proteins (20). Other activities of Gal-3 seem to involve sugar-independent interactions with a number of intracellular proteins including β-catenin (21), synexin (2), and K-Ras (4).

Many characteristics acquired by Gal-3 expression in cancer cells are also achievable by chronically active Ras proteins (8, 22). Similarly to Gal-3, Ras proteins can facilitate tumor cell growth, enhance tumor cell migration, and protect tumor cells from apoptotic stimuli (8, 23). Independent studies have recently shown a link between Gal-3 and Ras pathways (4) and showed that activation of ERK was required for Gal-3 suppression of cytotoxic drug–induced apoptosis in BT-549/Gal-3 cells (17). In spite of this knowledge, there is very little evidence concerning how Gal-3 carries out its related functions. The present study clearly shows that several functions of Gal-3 are, at least in part, a result of K-Ras activation. We show that K-Ras is drastically activated by Gal-3(wt) in BT-549 cells and this is accompanied by an increase in phospho-ERK. Furthermore, by using specific inhibitors for Ras or MEK (FTS or UO126 respectively), we show that stimulation of apoptotic activity, inhibition cell proliferation, and inhibition of anchorage-independent growth involve the K-Ras/MEK pathway. Accordingly, the two mutants of Gal-3 that lost their antiapoptotic function, as reported previously (1, 3), did not affect Ras proteins. Wild-type Gal-3 but not its inactive mutants coimmunoprecipitates and colocalizes with oncogenic GFP-K-Ras, suggesting that the lack of K-Ras activation by Gal-3 mutants is associated with the lack of their ability to interact, either directly or indirectly, with the GTP-bound K-Ras. Yet, we did not exclude the possibility that the lack of interaction of the Gal-3 mutants with K-Ras result from incorrect

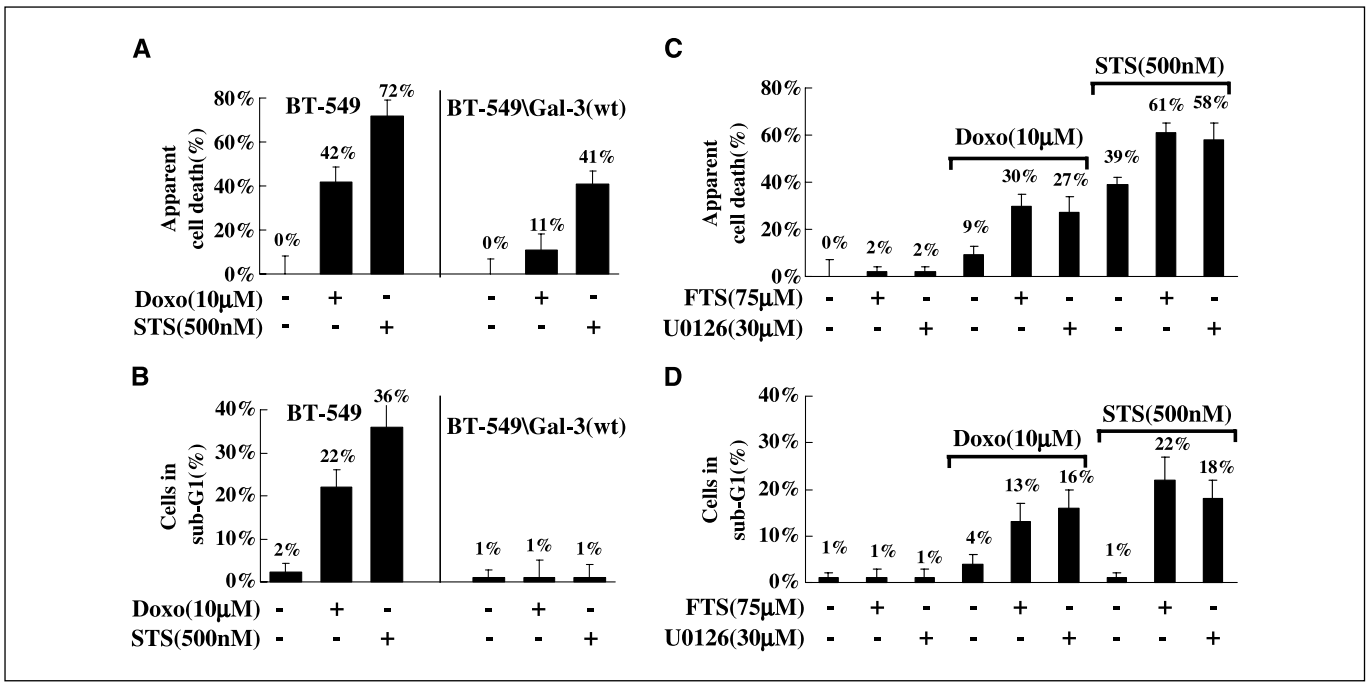

Figure 8. Ras- and MEK-dependent antiapoptotic activity of Gal-3. BT-549 and BT-549/Gal-3(wt) cells were preincubated for 10 hours with the Ras inhibitor (75 μmol/L) FTS (+) or the MEK inhibitor (30 μmol/L) UO126 (+) or vehicle (−). Apoptosis then induced by adding either 10 μmol/L Adriamycin (Doxo, +) or 500 nmol/L staurosporine (*STS*) (+) or vehicle as a control (−) for 12 or 36 hours, respectively. The viability of the cells was then measured using MTT assay and cell death was calculated as a percent of the untreated control cells (*A* and *C*). Cells sub-G_1 were monitored by flow cytometry analysis (*B* and *D*). Representative data from one of three similar experiments are shown. *Columns,* mean; *bars,* SD.

folding. In the case of the phosphorylation site, it is feasible to aim this question. Upcoming experiments should examine the importance of the Ser^6 phosphorylation state for interaction with K-Ras in the wt Gal-3 protein using *in vitro* assays. Nonetheless, our experiments strongly suggest that Gal-3/K-Ras binding promoted K-Ras activation, presumably by stabilizing K-Ras-GTP with the consequent activation of Raf-MEK-ERK signaling that is required for BT-549/Gal-3 cell transformation (17).

Intriguingly, we show here for the first time that Gal-3 induced a decrease in N-Ras-GTP levels in BT-549/Gal-3(wt) cells. In fact, Gal-3 expression resulted in a shift from mostly N-Ras usage in the parental BT-549 cells to mostly K-Ras usage in BT-549/Gal-3(wt) cells. Clearly, it is of importance to examine whether this act upon N-Ras is general or limited to this specific type of carcinoma cells. Furthermore, the mechanisms of N-Ras activation in the parental BT-549 cells and the mechanisms by which Gal-3 cancels N-Ras activation in these cells are not clear. It is possible that the high levels of N-Ras protein in BT-549 cells provide a driving force for strong RasGEF activity, perhaps for a selective activity of the N-Ras–specific GRP1 protein (24).

A number of mechanisms might account for the observed Gal-3–associated reduction in N-Ras-GTP levels in BT-549/Gal-3 cells. One mechanism could involve enhancement of GTP hydrolysis by a specific N-Ras GTPase activation protein; a second could involve inactivation of a specific N-RasGEF protein; a third mechanism could involve alteration in the subcellular localization of N-Ras. This possibility is consistent with recent studies that showed that Ras activation and signaling occurs not only in the cell membrane but also in various endomembranes, including Golgi and endoplasmic reticulum (25, 26). In addition, one would postulate that once Gal-3 binds to K-Ras-GTP, it forms a complex that is insensitive to Ras GTPase-activating proteins perhaps because the GTPase-activating protein domain in K-Ras protein is blocked by Gal-3. In turn, free GTPase-activating proteins that are no longer engaged with K-Ras may induce GTP hydrolysis of N-Ras. Last, it is also possible that specific K-Ras–Gal-3 signals are in charge of the GTP hydrolysis of N-Ras. Nonetheless, given that previous studies (4) have shown that Gal-3 binds to K-Ras, but not to other Ras isoforms, it is unlikely that Gal-3 interacts by itself with N-Ras and enhances its catalytic activity.

The shift from mostly N-Ras usage in the parental BT-549 cells to mostly K-Ras usage in the Gal-3–expressing cells was accompanied by a radical change in Ras signaling. Whereas the levels of phospho-ERK were increased, the levels of activity of two other canonical Ras downstream paths, namely PI3K/AKT and RalGEF/Ral, were remarkably reduced to undetectable levels. In light of recent studies showing preference of Ras isoforms toward Ras effectors (15, 27), it is tempting to speculate that PI3K and Ral pathways are selectively activated by N-Ras-GTP in BT-549 cells, whereas the Raf-MEK-ERK pathway is selectively activated by K-Ras-GTP in BT-549/Gal-3 cells. Accordingly, the elimination of GTP-N-Ras in BT-549/Gal-3 cells results in a decrease in the levels of activity of PI3K/AKT and Ral.

Finally, it is worth noting that this study shows that human tumors may acquire K-Ras–transforming characteristics without an activating mutation in the *K-ras* gene rather by elevated expression of Gal-3. Thus, inhibitors of both Gal-3 and of K-Ras could be useful for cancer therapy.

Acknowledgments

Received 3/9/2005; revised 5/15/2005; accepted 6/13/2005.

Grant support: NIH grant CA-46120 (A. Raz) and Israel Science Foundation grant 339/02-3 (Y. Kloog).

The costs of publication of this article were defrayed in part by the payment of page charges. This article must therefore be hereby marked *advertisement* in accordance with 18 U.S.C. Section 1734 solely to indicate this fact.

References

1. Yoshii T, Fukumori T, Honjo Y, Inohara H, Kim HR, Raz A. Galectin-3 phosphorylation is required for its anti-apoptotic function and cell cycle arrest. J Biol Chem 2002;277:6852–7.
2. Yu F, Finley RL Jr, Raz A, Kim HR. Galectin-3 translocates to the perinuclear membranes and inhibits cytochrome *c* release from the mitochondria. A role for synexin in galectin-3 translocation. J Biol Chem 2002; 277:15819–27.
3. Kim HR, Lin HM, Biliran H, Raz A. Cell cycle arrest and inhibition of anoikis by galectin-3 in human breast epithelial cells. Cancer Res 1999;59:4148–54.
4. Elad-Sfadia G, Haklai R, Balan E, Kloog Y. Galectin-3 augments K-Ras activation and triggers a Ras signal that attenuates ERK but not phosphoinositide 3-kinase activity. J Biol Chem 2004;279:34922–30.
5. Downward J. Role of receptor tyrosine kinases in G-protein-coupled receptor regulation of Ras: transactivation or parallel pathways? Biochem J 2003;376:e9–10.
6. Cox AD, Der CJ. The dark side of Ras: regulation of apoptosis. Oncogene 2003;22:8999–9006.
7. Downward J. Ras signalling and apoptosis. Curr Opin Genet Dev 1998;8:49–54.
8. Shields JM, Pruitt K, McFall A, Shaub A, Der CJ. Understanding Ras: 'it ain't over 'til it's over'. Trends Cell Biol 2000;10:147–54.
9. McFall A, Ulku A, Lambert QT, Kusa A, Rogers-Graham K, Der CJ. Oncogenic Ras blocks anoikis by activation of a novel effector pathway independent of phosphatidylinositol 3-kinase. Mol Cell Biol 2001;21:5488–99.
10. Shalom-Feuerstein R, Lindenboim L, Stein R, Cox AD, Kloog Y. Restoration of sensitivity to anoikis in Ras-transformed rat intestinal epithelial cells by a Ras inhibitor. Cell Death Differ 2004;11:244–7.
11. Niv H, Gutman O, Henis YI, Kloog Y. Membrane interactions of a constitutively active GFP-Ki-Ras 4B and their role in signaling. Evidence from lateral mobility studies. J Biol Chem 1999;274:1606–13.
12. Paz A, Haklai R, Elad-Sfadia G, Ballan E, Kloog Y. Galectin-1 binds oncogenic H-Ras to mediate Ras membrane anchorage and cell transformation. Oncogene 2001;20:7486–93.
13. Pardo OE, Arcaro A, Salerno G, Raguz S, Downward J, Seckl MJ. Fibroblast growth factor-2 induces translational regulation of Bcl-XL and Bcl-2 via a MEK-dependent pathway: correlation with resistance to etoposide-induced apoptosis. J Biol Chem 2002;277: 12040–6.
14. Hall A. The cellular functions of small GTP-binding proteins. Science 1990;249:635–40.
15. Wolfman A. Ras isoform-specific signaling: location, location, location. Sci STKE 2001;2001:PE2.
16. Takenaka Y, Fukumori T, Raz A. Galectin-3 and metastasis. Glycoconj J 2004;19:543–9.
17. Takenaka Y, Fukumori T, Yoshii T, et al. Nuclear export of phosphorylated galectin-3 regulates its anti-apoptotic activity in response to chemotherapeutic drugs. Mol Cell Biol 2004;24:4395–406.
18. Gana-Weisz M, Halaschek-Wiener J, Jansen B, Elad G, Haklai R, Kloog Y. The Ras inhibitor *S-trans,trans*-farnesylthiosalicylic acid chemosensitizes human tumor cells without causing resistance. Clin Cancer Res 2002;8: 555–65.
19. Halaschek-Wiener J, Kloog Y, Wacheck V, Jansen B. Farnesyl thiosalicylic acid chemosensitizes human melanoma *in vivo*. J Invest Dermatol 2003;120:109–15.
20. Liu FT, Patterson RJ, Wang JL. Intracellular functions of galectins. Biochim Biophys Acta 2002;1572:263–73.
21. Shimura T, Takenaka Y, Tsutsumi S, Hogan V, Kikuchi A, Raz A. Galectin-3, a novel binding partner of β-catenin. Cancer Res 2004;64:6363–7.
22. Downward J. Targeting RAS signalling pathways in cancer therapy. Nat Rev Cancer 2003;3:11–22.
23. Hancock JF. Ras proteins: different signals from different locations. Nat Rev Mol Cell Biol 2003;4: 373–84.
24. Jones MK, Jackson JH. Ras-GRF activates Ha-Ras, but not N-Ras or K-Ras 4B, protein *in vivo*. J Biol Chem 1998; 273:1782–7.
25. Bivona TG, Philips MR. Ras pathway signaling on endomembranes. Curr Opin Cell Biol 2003;15:136–42.
26. Chiu VK, Bivona T, Hach A, et al. Ras signalling on the endoplasmic reticulum and the Golgi. Nat Cell Biol 2002;4:343–50.
27. Yan J, Roy S, Apolloni A, Lane A, Hancock JF. Ras isoforms vary in their ability to activate Raf-1 and phosphoinositide 3-kinase. J Biol Chem 1998;273: 24052–6.